



2 Reconstruction of solar UV irradiance since 1974

3 N. A. Krivova,¹ S. K. Solanki,^{1,2} T. Wenzler,^{1,3} and B. Podlipnik¹

4 Received 30 April 2009; revised 25 June 2009; accepted 7 July 2009; published XX Month 2009.

5 [1] Variations of the solar UV irradiance are an important driver of chemical and physical
6 processes in the Earth's upper atmosphere and may also influence global climate. Here
7 we reconstruct solar UV irradiance in the range 115–400 nm over the period 1974–2007
8 by making use of the recently developed empirical extension of the Spectral And
9 Total Irradiance Reconstruction (SATIRE) models employing Solar Ultraviolet Spectral
10 Irradiance Monitor (SUSIM) data. The evolution of the solar photospheric magnetic flux,
11 which is a central input to the model, is described by the magnetograms and
12 continuum images recorded at the Kitt Peak National Solar Observatory between 1974 and
13 2003 and by the Michelson Doppler Imager instrument on SOHO since 1996. The
14 reconstruction extends the available observational record by 1.5 solar cycles. The
15 reconstructed Ly- α irradiance agrees well with the composite time series by Woods et al.
16 (2000). The amplitude of the irradiance variations grows with decreasing wavelength
17 and in the wavelength regions of special interest for studies of the Earth's climate (Ly- α
18 and oxygen absorption continuum and bands between 130 and 350 nm) is 1–2 orders
19 of magnitude stronger than in the visible or if integrated over all wavelengths (total solar
20 irradiance).

21 **Citation:** Krivova, N. A., S. K. Solanki, T. Wenzler, and B. Podlipnik (2009), Reconstruction of solar UV irradiance since 1974,
22 *J. Geophys. Res.*, 114, XXXXXX, doi:10.1029/2009JD012375.

24 1. Introduction

25 [2] Solar irradiance variations show a strong wavelength
26 dependence. Whereas the total (integrated over all wave-
27 lengths) solar irradiance (TSI) changes by about 0.1% over
28 the course of the solar cycle, the irradiance in the UV part of
29 the solar spectrum varies by up to 10% in the 150–300 nm
30 range and by more than 50% at shorter wavelengths, includ-
31 ing the Ly- α emission line near 121.6 nm [e.g., Floyd et al.,
32 2003a]. On the whole, more than 60% of the TSI variations
33 over the solar cycle are produced at wavelengths below
34 400 nm [Krivova et al., 2006; cf. Harder et al., 2009].

35 [3] These variations may have a significant impact on the
36 Earth's climate system. Ly- α , the strongest line in the solar
37 UV spectrum, which is formed in the transition region and
38 the chromosphere, takes an active part in governing the
39 chemistry of the Earth's upper stratosphere and mesosphere,
40 for example, by ionizing nitric oxide, which affects the
41 electron density distribution, or by stimulating dissociation
42 of water vapor and producing chemically active HO(x) that
43 destroy ozone [e.g., Frederick, 1977; Brasseur and Simon,
44 1981; Huang and Brasseur, 1993; Fleming et al., 1995;
45 Egorova et al., 2004; Langematz et al., 2005a]. Also,
46 radiation in the Herzberg oxygen continuum (200–
47 240 nm) and the Schumann-Runge bands of oxygen

(180–200 nm) is important for photochemical ozone 48
production [e.g., Haigh, 1994, 2007, accessed March 49
2009; Egorova et al., 2004; Langematz et al., 2005b; Rozanov 50
et al., 2006; Austin et al., 2008]. UV radiation in the wave- 51
length range 200–350 nm, i.e., around the Herzberg oxygen 52
continuum and the Hartley-Huggins ozone bands, is the main 53
heat source in the stratosphere and mesosphere [Haigh, 1999, 54
2007; Rozanov et al., 2004, 2006]. 55

[4] The record of regular measurements of the solar UV 56
irradiance spectrum, accurate enough to assess its varia- 57
tions, goes back to 1991, when the Upper Atmosphere 58
Research Satellite (UARS) was launched. Among others, 59
it carried two instruments for monitoring solar radiation in 60
the UV, the Solar Ultraviolet Spectral Irradiance Monitor 61
(SUSIM) [Brueckner et al., 1993] and the Solar Stellar 62
Irradiance Comparison Experiment (SOLSTICE) [Rottman 63
et al., 1993]. These data sets are of inestimable value, but 64
remain too short to allow reliable evaluation of solar 65
influence on the Earth's climate and need to be extended 66
back in time with the help of models. 67

[5] Reconstructions of solar UV irradiance have earlier 68
been presented by Fligge and Solanki [2000] and by Lean 69
[2000]. The first one was based on LTE (Local Thermo- 70
dynamic Equilibrium) calculations of the solar spectrum and 71
the latter on UARS/SOLSTICE measurements. The LTE 72
approximation gives inaccurate results below approximately 73
200 nm and in some spectral lines, whereas the long- 74
term uncertainty of SOLSTICE (as well as of all other 75
instruments that measured solar UV irradiance before 76
SORCE) exceeded the solar cycle variation above approxi- 77
mately 250 nm, thus leading to incorrect estimates of the UV 78

¹Max-Planck-Institut für Sonnensystemforschung, Katlenburg-Lindau, Germany.

²School of Space Research, Kyung Hee University, Yongin, South Korea.

³Hochschule für Technik Zürich, Zurich, Switzerland.

79 irradiance variability at longer wavelengths [see *Lean et al.*,
80 2005; *Krivova et al.*, 2006].

81 [6] Whereas considerable advance has recently been
82 made in modeling the variations of the total solar irradiance
83 and the irradiance at wavelengths longer than about 300 nm
84 [e.g., *Unruh et al.*, 1999; *Ermolli et al.*, 2003; *Krivova et al.*,
85 2003; *Wenzler et al.*, 2004, 2005, 2006], models at shorter
86 wavelengths have not kept pace. This is because the
87 LTE approximation usually taken in calculations of the
88 brightness of different photospheric components fails in
89 this wavelength range and non-LTE calculations are much
90 more arduous [e.g., *Fontenla et al.*, 1999, 2006; *Haberreiter*
91 *et al.*, 2005].

92 [7] An alternative approach has been developed by
93 *Krivova and Solanki* [2005a] and *Krivova et al.* [2006] that
94 allows an empirical extrapolation of the successful Spectral
95 and Total Irradiance Reconstruction (SATIRE) models
96 [*Krivova and Solanki*, 2005b; *Solanki et al.*, 2005] down
97 to 115 nm using available SUSIM measurements. *Krivova*
98 *et al.* [2006] have combined this technique with the model
99 of *Krivova et al.* [2003] to reconstruct the variations of the
100 solar UV irradiance over the period 1996–2002, i.e., the
101 rising phase of cycle 23, using MDI (Michelson Doppler
102 Imager on SOHO) [*Scherrer et al.*, 1995] magnetograms
103 and continuum images. Here we employ the data from the
104 National Solar Observatory Kitt Peak (NSO KP), in order to
105 reconstruct the solar UV irradiance spectrum back to 1974.
106 We then combine this KP-based reconstruction for the
107 period 1974–2002 with the reconstruction based on MDI
108 data [*Krivova et al.*, 2006], which has now been extended to
109 2006. In order to fill in the gaps in daily data and to extend
110 the time series to 2007, when MDI continuum images
111 displayed deteriorating quality, we employ the Mg II core-
112 to-wing ratio and the solar F10.7 cm radio flux. Hence the
113 present paper extends the work of *Krivova et al.* [2006] to
114 three cycles, i.e., the whole period of time over which high-
115 quality magnetograms are available.

116 [8] The model is described in section 2, the results are
117 presented in section 3 and summarized in section 4.

118 2. Model

119 [9] We take a similar approach as *Krivova et al.* [2006].
120 This means that variations of the solar total and spectral
121 irradiance on time scales of days to decades are assumed to
122 be entirely due to the evolution of the solar surface magnetic
123 field. Under this assumption, *Krivova et al.* [2003] and
124 *Wenzler et al.* [2005, 2006] have successfully modeled the
125 observed variations of the total solar irradiance. *Krivova et*
126 *al.* [2006] showed that this (SATIRE) model also works
127 well in the spectral range 220–240 nm (hereinafter, the
128 reference range). They then analyzed SUSIM data and
129 worked out empirical relationships between the irradiance
130 in this range and irradiances at all other wavelengths
131 covered by the SUSIM detectors (115–410 nm). Thus if
132 the irradiance in the range 220–240 nm is known, it is also
133 possible to calculate irradiance at other wavelengths in the
134 UV down to 115 nm.

135 2.1. Solar Irradiance at 220–240 nm

136 [10] In a first step, we apply the SATIRE model [*Solanki*
137 *et al.*, 2005; *Krivova and Solanki*, 2008] to NSO KP

magnetograms and continuum images, in order to recon- 138
struct solar irradiance in the reference range for the period 139
1974–2003. In SATIRE, the solar photosphere is divided 140
into four components: the quiet Sun, sunspot umbrae, 141
sunspot penumbrae and bright magnetic features (describing 142
both faculae and the network). Each component is described 143
by the time-independent spectrum calculated from the 144
corresponding model atmospheres in the LTE approxima- 145
tion [*Unruh et al.*, 1999]. Since the distribution of the 146
magnetic field on the solar surface evolves continuously, 147
the area covered by each of the components on the visible 148
solar disc also changes. This is represented by the 149
corresponding filling factors, which are retrieved from 150
the magnetograms and continuum images. In the period 151
1974–2003, such data were recorded (nearly daily) with the 152
512-channel Diode Array Magnetograph (before 1992) 153
[*Livingston et al.*, 1976] and the Spectromagnetograph 154
(after 1992) [*Jones et al.*, 1992] on Kitt Peak [see also 155
Wenzler et al., 2006]. Since 1996 magnetograms and 156
continuum images were also recorded by the MDI instru- 157
ment on SOHO. More details about the SATIRE model 158
have been given by *Fligge et al.* [2000], *Krivova et al.* 159
[2003], and *Wenzler et al.* [2005, 2006]. 160

[11] This model has one free parameter, B_{sat} , denoting the 161
field strength below which the facular contrast is propor- 162
tional to the magnetogram signal, while it is independent 163
(saturated) above that. It depends on the quality (noise level 164
and spatial resolution) of the employed magnetograms. 165
From a comparison with the PMOD composite [*Fröhlich*, 166
2006] of the TSI measurements, *Wenzler et al.* [2006, 2009] 167
found the value of $B_{\text{sat}} = 320$ G for the KP data, whereas 168
Krivova et al. [2003] obtained a value of $B_{\text{sat}} = 280$ G for 169
the MDI data. In this work we use the same values of this 170
parameter and do not vary them any more in order to fit the 171
spectral data. 172

[12] The solar irradiance integrated over the wavelength 173
range 220–240 nm reconstructed from the KP magneto- 174
grams and continuum images is shown in Figure 1 by the 175
red pluses connected by the dashed line where there are no 176
gaps in the daily sequence of data. The measurements by the 177
SUSIM instrument are represented by the green line. We use 178
daily level 3BS V22 data with a sampling of 1 nm [*Floyd et* 179
al., 2003b; L. Floyd, personal communication, 2007]. A 180
similar plot obtained with MDI data was given by *Krivova* 181
et al. [2006]. The apparent change in the behavior between 182
cycles 22 and 23 seen in Figure 1a is due to the incorrect 183
estimate of the degradation during the solar minimum 184
period (L. Floyd, personal communication, 2007). This is, 185
for example, confirmed by a comparison with the Mg II 186
core-to-wing ratio, which is free of such problems, and is 187
discussed in more detail by *Krivova et al.* [2006]. The 188
fact that a single shift in absolute values applied to the 189
SUSIM data before 1996 is sufficient in order to bring the 190
data in agreement with the model also supports this 191
conjecture. Indeed, in Figure 1b the period before 1996 is 192
shown on an enlarged scale. Here the measurements by 193
SUSIM were shifted in the absolute level by a fixed value 194
($-5.0 \times 10^6 \text{ W m}^{-3} \text{ nm}$), and a good correspondence 195
between the model and the data is seen. 196

[13] This is also demonstrated by Figure 2, where the 197
measured irradiance at 220–240 nm is plotted against the 198
modeled values. Dots and pluses are used for the data from 199

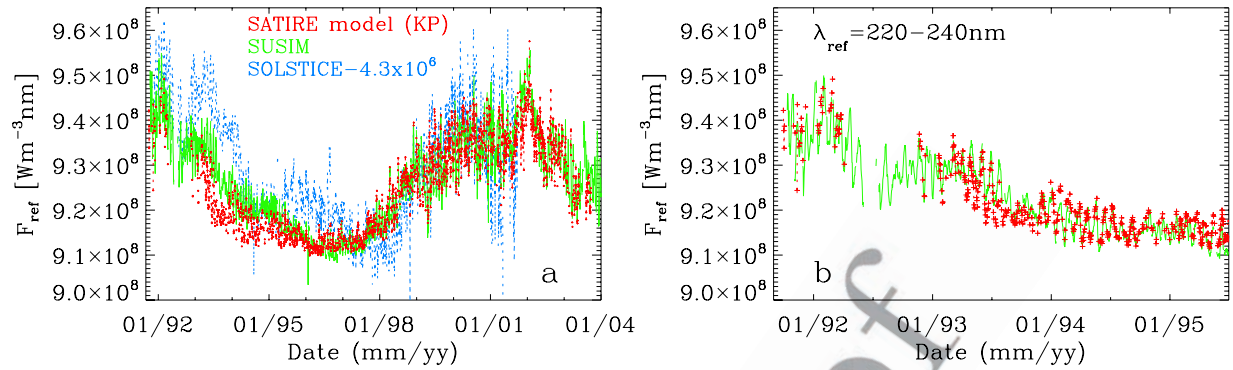


Figure 1. (a) Solar irradiance integrated over the wavelength range 220–240 nm as a function of time for the period 1991–2003. The green line shows SUSIM measurements [Floyd *et al.*, 2003b], and the red pluses (connected by the dashed line where there are no gaps) show the values reconstructed using SATIRE models and KP magnetograms. SOLSTICE data [Woods *et al.*, 1996] shifted by $-4.3 \times 10^6 \text{ W m}^{-3} \text{ nm}$ are shown by the blue dashed line. (b) Enlargement of Figure 1a restricted to the period before 1996 showing only SUSIM data and the reconstruction. Here SUSIM data were shifted by $-5.0 \times 10^6 \text{ W m}^{-3} \text{ nm}$.

cycles 22 and 23, respectively (no correction to the absolute level has been applied). The dashed straight line with a slope of 0.95 represents the regression to all points. The correlation coefficient is 0.93. The solid line with a slope of 1.02 is the regression to the cycle 23 data only. It is hardly distinguishable from the thick dotted line with a slope of 1.0 expected for a perfect fit. The corresponding correlation coefficient is 0.94, i.e., the same as found by Wenzler *et al.* [2006] for the modeled TSI compared to the PMOD composite for the period since 1992. We stress that the value of the free parameter, B_{sat} , was the same in both cases. This means that SATIRE reproduces independent SUSIM data without any further adjustments, which is yet another success of the model.

[14] In Figure 1a, we also plot SOLSTICE data [Woods *et al.*, 1996] represented by the blue dashed line. Note that for comparison sake the SOLSTICE absolute values have been

shifted by $-4.3 \times 10^6 \text{ W m}^{-3} \text{ nm}$. It is clear that at 220–240 nm the model is in a better agreement with the SUSIM data, even if the correction due to the degradation is not taken into account, than with the measurements by SOLSTICE, which also show a higher scatter.

[15] Solar irradiance in the reference range for the period 1996–2002 was also reconstructed by Krivova *et al.* [2006, Figure 2] using MDI magnetograms and continuum images. We have updated their model through the beginning of 2006 and combined it with the KP-based reconstruction shown in Figure 1. On the days when both models are available, the preference was given to the MDI-based values, since they were found to be more accurate [cf. Krivova *et al.*, 2003; Wenzler *et al.*, 2004, 2006].

[16] Unfortunately, the flat field distortion progressively affecting MDI continuum images requires a correction of all images recorded after approximately 2005 before they can

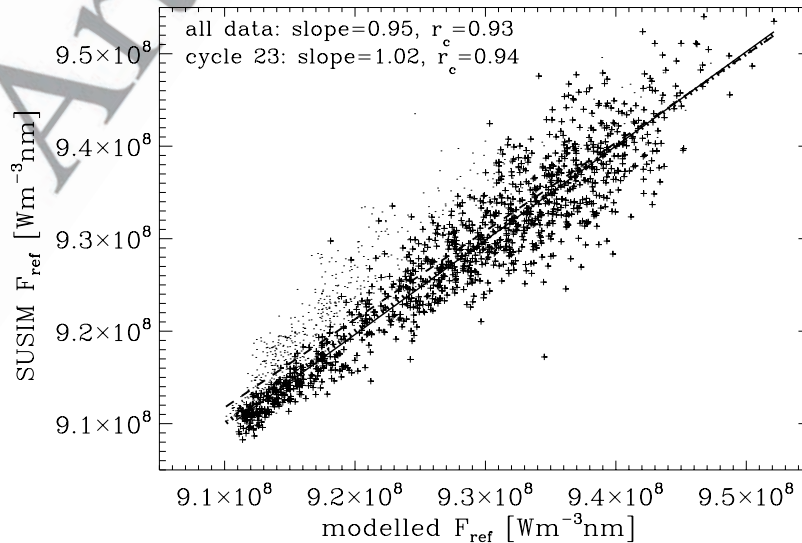


Figure 2. Solar irradiance in the range 220–240 nm as measured by SUSIM versus reconstructed by SATIRE. Dots and pluses are used for cycles 22 and 23, respectively. The dashed straight line is the regression to all points (with no correction applied to SUSIM's absolute level). The solid line is the regression for cycle 23 only. The thick dotted line almost coinciding with the solid line shows the expectation value, i.e., a slope of 1.0 and no offset. Correlation coefficients and slopes are indicated.

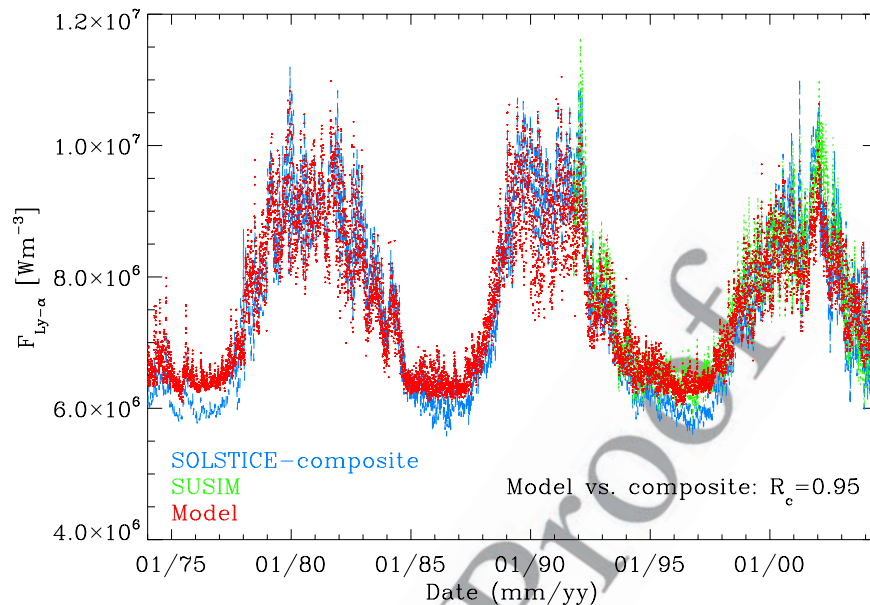


Figure 3. Solar Ly- α irradiance since 1974 reconstructed by SATIRE (red), measured by the SUSIM instrument (green), and compiled by *Woods et al.* [2000] (blue).

234 be employed for the irradiance reconstructions. Such a
 235 correction is being attempted, but the outcome is not certain
 236 and it seems advisable to complete the reconstruction
 237 instead of waiting an unknown length of time.

238 [17] There are also some gaps in the daily reconstructions,
 239 when no magnetograms and continuum images were
 240 recorded, in particular, in the 1970s. On the other hand,
 241 climate models often require solar signal input with a daily
 242 cadence. Therefore, we have employed the Mg II core-to-
 243 wing ratio [*Viereck et al.*, 2004] and the solar F10.7 cm
 244 radio flux [*Tanaka et al.*, 1973] in order to fill in the gaps
 245 and to extend the data to 2007. This has been done by using
 246 a linear regression between the irradiance in the reference
 247 range (220–240 nm) and the Mg II index (the linear
 248 correlation coefficient is $R_c = 0.98$) and a quadratic rela-
 249 tionship between the irradiance in the reference range and
 250 the F10.7 flux ($R_c = 0.92$). Mg II and F10.7 cm flux data are
 251 obtained from the National Geophysical Data Center
 252 (NGDC; <http://www.ngdc.noaa.gov/ngdc.html>).

253 2.2. UV Spectral Irradiance

254 [18] In order to extrapolate the SATIRE model based on
 255 KP NSO and MDI magnetograms and continuum images to
 256 other UV wavelengths, we made use of the relations
 257 between irradiances, F_λ , at a given wavelength, λ , and in
 258 the reference interval, F_{ref} (220–240 nm). These relation-
 259 ships in the range 115–410 nm were deduced by *Krivova et*
 260 *al.* [2006] using daily SUSIM data recorded between 1996
 261 and 2002. We have repeated this analysis with the data set
 262 extended to 2005, but did not find any significant difference
 263 to the earlier derived values and therefore employed the
 264 relationships from the previous work for consistency.

265 [19] Using the calculated irradiances at 220–240 nm and
 266 empirical relationships F_λ/F_{ref} versus F_{ref} , solar UV irradiance
 267 at 115–270 nm was reconstructed for the whole period
 268 1974–2007. Since the long-term uncertainty of SUSIM
 269 measurements becomes comparable to or higher than the

solar cycle variation at around 250 and 300 nm, respectively
 [Woods *et al.*, 1996; Floyd *et al.*, 2003b], above 270 nm
 SATIRE is found to be more accurate than the measure-
 ments [*Krivova et al.*, 2006; cf. *Unruh et al.*, 2008],
 Therefore spectral irradiance values at these wavelengths
 are calculated directly from SATIRE.

277 3. Results

278 3.1. Ly- α Irradiance

279 [20] The Ly- α line is of particular interest not just for its
 280 prominence in the solar spectrum and its importance for the
 281 Earth's upper atmosphere, but also because for this line a
 282 composite of measurements is available for the whole
 283 period considered here. In Figure 3 we compare the recon-
 284 structed solar Ly- α irradiance (red) with the composite time
 285 series (blue) compiled by *Woods et al.* [2000]. The latter
 286 record comprises the measurements from the Atmospheric
 287 Explorer E (AE-E, 1977–1980), the Solar Mesosphere
 288 Explorer (SME, 1981–1989), UARS SOLSTICE (1991–
 289 2001), and the Solar EUV Experiment (SEE) on TIMED
 290 (Thermosphere, Ionosphere, Mesosphere Energetics and
 291 Dynamic Mission launched in 2001). The gaps are filled
 292 in using proxy models based on Mg core-to-wing and F10.7
 293 indices, and the F10.7 model is also used to extrapolate the
 294 data set back in time. The UARS SOLSTICE data are used
 295 as the reference, and other measurements and the models are
 296 adjusted to the SOLSTICE absolute values. Although this
 297 time series is thus only partly based on direct Ly- α
 298 observations, it is the nearest we found to an observational
 299 time series to compare our model with.

300 [21] For comparison, the SUSIM measurements are also
 301 plotted in Figure 3 (green). The model agrees well with the
 302 SUSIM data, which confirms that our semiempirical tech-
 303 nique works well. Note that there is no change in the
 304 behavior around the minimum in 1996. This is yet another
 305 indication of the instrumental origin of the jump in the

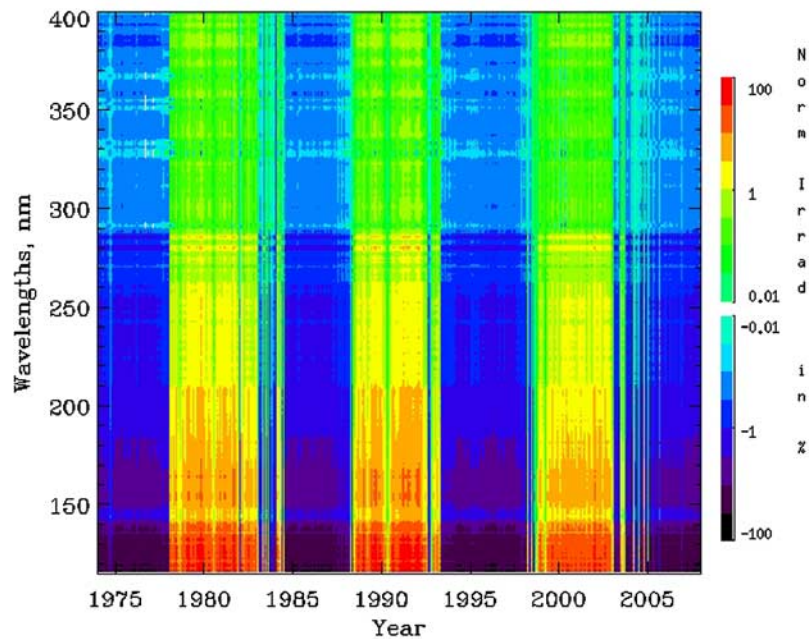


Figure 4. Reconstructed solar UV irradiance at 115–400 nm in the period 1974–2007 normalized to the mean at each wavelength over the whole period of time.

306 absolute values seen in SUSIM's irradiances at 220–240
307 and many other wavelengths [see *Krivova et al.*, 2006].

308 [22] As Figure 3 shows, there is some difference (about
309 5%) in the magnitude of the Ly- α solar cycle variations
310 between SOLSTICE and SUSIM. Since our model agrees
311 with SUSIM (by construction), a difference of this magnitude
312 remains also between our model and SOLSTICE. Other than
313 that, the model agrees with the completely independent
314 composite time series very well, with a correlation coefficient
315 of 0.95 (remember that the free parameter of the SATIRE
316 model was fixed from a comparison with the PMOD com-
317 posite of the TSI and not varied to fit the UV data).

318 [23] The solar Ly- α irradiance has also been modeled by
319 *Haberreiter et al.* [2005] using the filling factors derived
320 from the MDI and KP NSO magnetograms and continuum
321 images in combination with the brightness spectra for the
322 quiet Sun, sunspots and faculae calculated with their NLTE
323 code COSI. The calculated variability was about a factor of
324 2 lower than the measured one. NLTE calculation are, in
325 principal, better suitable for calculations of the solar UV
326 irradiance and they have recently made significant progress
327 [e.g., *Fontenla et al.*, 2006, 2007; *Haberreiter et al.*, 2008].
328 Their complexity and the number of processes to be
329 accounted for do not, however, as yet allow an accurate
330 reconstruction of the solar spectral irradiance over broader
331 spectral ranges and longer periods of time.

332 3.2. Solar UV Irradiance at 115–400 nm in 1974–2007

333 [24] Figure 4 shows the reconstructed solar UV irradiance
334 in the range 115–400 nm over the period 1974–2007 (i.e.,
335 covering cycles 21–23), normalized to the mean at each
336 wavelengths over the complete time period. At all considered
337 wavelengths, the irradiance changes in phase with the solar
338 cycle, in agreement with recent results based on 4 years
339 of SIM/SORCE measurements [*Harder et al.*, 2009]. The
340 variability becomes significantly stronger toward shorter

wavelengths: from about 1% over the activity cycle at around
300 nm to more than 100% in the vicinity of Ly- α .

342 [25] Figure 5 shows the solar UV irradiance integrated
343 over spectral ranges of particular interest for climate studies
344 as a function of time: 130–175 nm (Figure 5a), 175–200 nm
345 (Figure 5b), 200–242 nm (Figure 5c), and 200–350 nm
346 (Figure 5d). Solar radiation at 130–175 nm (Schumann-
347 Runge continuum) is completely absorbed in the thermo-
348 sphere. Over activity cycles 21–23, solar radiative flux in
349 this spectral range varied by about 10–15% (Figure 5a), i.e.,
350 by more than a factor of 100 more than solar cycle
351 variations in the solar total energy flux (total solar irradi-
352 ance). In the oxygen Schumann-Runge bands (175–200 nm)
353 and Herzberg continuum (200–242 nm), important for
354 photochemical ozone production and destruction in the
355 stratosphere and mesosphere, solar irradiance varied on
356 average by about 5–8% (Figure 5b) and 3% (Figure 5c),
357 respectively. In the Hartley-Huggins ozone bands between
358 200 and 350 nm, solar radiation is the main heat source in
359 the stratosphere. At these wavelengths, the amplitude of the
360 solar cycle variation is of the order of 1%, which is still an
361 order of magnitude stronger than variations of the total solar
362 irradiance.

363 [26] The complete data set of the reconstructed solar irradi-
364 ance at 115–400 nm over the period 1974–2007 is available
365 as auxiliary material and at [http://www.mps.mpg.de/projects/](http://www.mps.mpg.de/projects/sun-climate/data.html)
366 [sun-climate/data.html](http://www.mps.mpg.de/projects/sun-climate/data.html).¹
367

369 4. Summary

370 [27] *Krivova et al.* [2006] have developed an empirical
371 technique, which allows an extrapolation of the
372 magnetogram-based reconstructions of solar total and spectral

¹Auxiliary materials are available at <ftp://ftp.agu.org/apend/jd/2009/jd012375>.

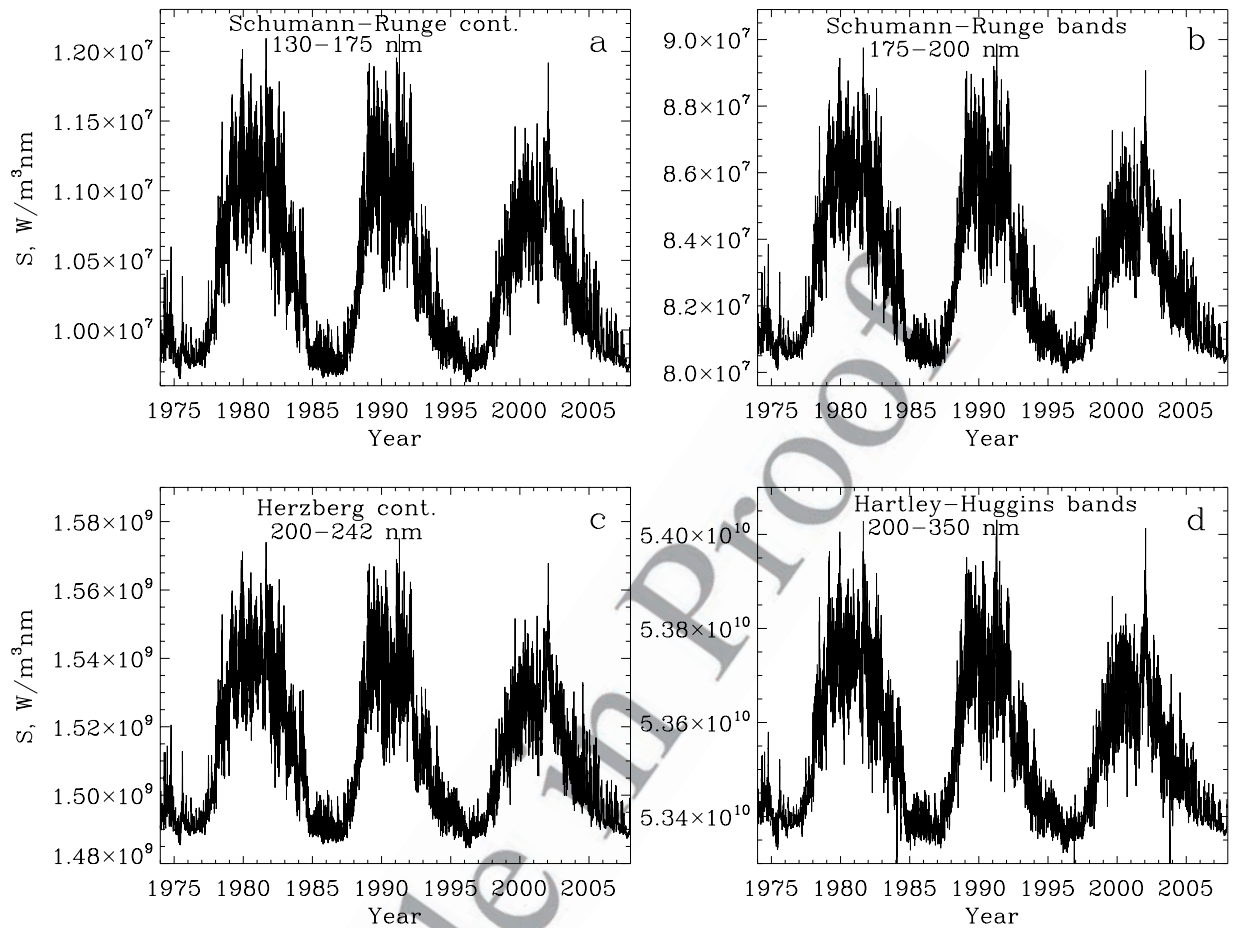


Figure 5. Reconstructed solar irradiance in the period 1974–2007 integrated over the wavelength ranges (a) 130–175 nm (Schumann-Runge continuum), (b) 175–200 nm (Schumann-Runge bands), (c) 200–242 nm (Herzberg continuum), and (d) 200–350 nm (Hartley-Huggins bands).

376 irradiance to shorter wavelengths, down to 115 nm.
 377 They applied this technique to obtain variations of solar UV
 378 irradiance between 1996 and 2002. We have now extended
 379 their model to both earlier and more recent times. Thus we
 380 provide a reconstruction of the solar UV irradiance spectrum
 381 between 115 and 400 nm over the period 1974–2007. This
 382 extends the available observational record by about 1.5 solar
 383 cycles, i.e., roughly doubles the available record.

384 [28] As a test of the quality of our model, we have
 385 compared the reconstructed solar Ly- α irradiance with the
 386 completely independent composite of measurements and
 387 proxy models by *Woods et al.* [2000]. There is a small
 388 (about 5%) difference in the solar cycle amplitude between
 389 our model and that composite. This difference is also
 390 present between the SUSIM and SOLSTICE data, which
 391 are the reference sets for the model and the composite,
 392 respectively. Aside from that, the modeled and composite
 393 records closely agree with each other.

394 [29] Solar UV irradiance varies in phase with the solar
 395 cycle at all wavelengths between 115 and 400 nm, in
 396 agreement with the recent finding of *Harder et al.* [2009]
 397 based on SIM/SORCE measurements over 2004–2007. The
 398 relative amplitude of the variations grows with decreasing
 399 wavelength. In the wavelength regions important for studies
 400 of the Earth’s climate (e.g., Ly- α and oxygen absorption
 401 continuum and bands between 130 and 350 nm), the relative

variation is 1–2 orders of magnitude stronger than in the
 visible or if integrated over all wavelengths (i.e., TSI).

[30] SATIRE-based reconstructed UV irradiance in the
 spectral range 115–400 nm between 1 January 1974 and
 31 December 2007 is available as auxiliary material and at
<http://www.mps.mpg.de/projects/sun-climate/data.html>.

[31] **Acknowledgments.** We thank L. Floyd for providing SUSIM
 data and valuable comments and V. Holzwarth for helpful discussions. The
 composite Lyman α time series was retrieved from the LASP ftp server
 (ftp://laspftp.colorado.edu). This work was supported by the Deutsche
 Forschungsgemeinschaft, DFG project SO 711/2 and by the WCU grant
 R31-10016 funded by the Korean Ministry of Education, Science and
 Technology. We also thank the International Space Science Institute (Bern)
 for giving us the opportunity to discuss this work with the great interna-
 tional team on “Interpretation and modeling of SSI measurements.”

References

- Austin, J., et al. (2008), Coupled chemistry climate model simulations of
 the solar cycle in ozone and temperature, *J. Geophys. Res.*, *113*, D11306,
 doi:10.1029/2007JD009391.
 Brasseur, G., and P. C. Simon (1981), Stratospheric chemical and thermal
 response to long-term variability in solar UV irradiance, *J. Geophys. Res.*,
86, 7343–7362.
 Brueckner, G. E., K. L. Edlow, L. E. Floyd, J. L. Lean, and M. E. Vanhoosier
 (1993), The solar ultraviolet spectral irradiance monitor (SUSIM) experiment
 on board the Upper Atmosphere Research Satellite (UARS), *J. Geophys.*
Res., *98*, 10,695–10,711.
 Egorova, T., E. Rozanov, E. Manzini, M. Haberreiter, W. Schmutz,
 V. Zubov, and T. Peter (2004), Chemical and dynamical response to the
 11-year variability of the solar irradiance simulated with a chemistry-

- 431 climate model, *Geophys. Res. Lett.*, *31*, L06119, doi:10.1029/
432 2003GL019294.
- 433 Ermolli, I., F. Berrilli, and A. Florio (2003), A measure of the network
434 radiative properties over the solar activity cycle, *Astron. Astrophys.*, *412*,
435 857–864.
- 436 Fleming, E. L., S. Chandra, C. H. Jackman, D. B. Considine, and A. R.
437 Douglass (1995), The middle atmospheric response to short and long
438 term solar UV variations: Analysis of observations and 2D model results,
439 *J. Atmos. Terr. Phys.*, *57*, 333–365.
- 440 Fligge, M., and S. K. Solanki (2000), The solar spectral irradiance since
441 1700, *Geophys. Res. Lett.*, *27*, 2157–2160.
- 442 Fligge, M., S. K. Solanki, and Y. C. Unruh (2000), Modelling irradiance
443 variations from the surface distribution of the solar magnetic field,
444 *Astron. Astrophys.*, *353*, 380–388.
- 445 Floyd, L., G. Rottman, M. DeLand, and J. Pap (2003a), 11 years of solar
446 UV irradiance measurements from UARS, *Eur. Space Agency Spec.
447 Publ.*, *ESA SP-535*, 195–203.
- 448 Floyd, L. E., J. W. Cook, L. C. Herring, and P. C. Crane (2003b), SUSIM'S
449 11-year observational record of the solar UV irradiance, *Adv. Space Res.*,
450 *31*, 2111–2120.
- 451 Fontenla, J., O. R. White, P. A. Fox, E. H. Avrett, and R. L. Kurucz (1999),
452 Calculation of solar irradiances. I. Synthesis of the solar spectrum,
453 *Astrophys. J.*, *518*, 480–499.
- 454 Fontenla, J. M., E. Avrett, G. Thuillier, and J. Harder (2006), Semiempirical
455 models of the solar atmosphere. I. The quiet- and active Sun photosphere
456 at moderate resolution, *Astrophys. J.*, *639*, 441–458.
- 457 Fontenla, J. M., K. S. Balasubramaniam, and J. Harder (2007), Semiempirical
458 models of the solar atmosphere. II. The quiet-Sun low chromosphere at
459 moderate resolution, *Astrophys. J.*, *667*, 1243–1257.
- 460 Frederick, J. E. (1977), Chemical response of the middle atmosphere to
461 changes in the ultraviolet solar flux, *Planet. Space Sci.*, *25*, 1–4.
- 462 Fröhlich, C. (2006), Solar irradiance variability since 1978: Revision of the
463 PMOD composite during solar cycle 21, *Space Sci. Rev.*, *125*, 53–65.
- 464 Haberreiter, M., N. A. Krivova, W. Schmutz, and T. Wenzler (2005),
465 Reconstruction of the solar UV irradiance back to 1974, *Adv. Space
466 Res.*, *35*, 365–369.
- 467 Haberreiter, M., W. Schmutz, and I. Hubeny (2008), NLTE model calcula-
468 tions for the solar atmosphere with an iterative treatment of opacity
469 distribution functions, *Astron. Astrophys.*, *492*, 833–840.
- 470 Haigh, J. D. (1994), The role of stratospheric ozone in modulating the solar
471 radiative forcing of climate, *Nature*, *370*, 544–546.
- 472 Haigh, J. D. (1999), Modelling the impact of solar variability on climate,
473 *J. Atmos. Terr. Phys.*, *61*, 63–72.
- 474 Haigh, J. D. (2007), The Sun and the Earth's climate, *Living Rev. Sol. Phys.*,
475 *2*, lrsp-2007-2.
- 476 Harder, J. W., J. M. Fontenla, P. Pilewskie, E. C. Richard, and T. N. Woods
477 (2009), Trends in solar spectral irradiance variability in the visible and
478 infrared, *Geophys. Res. Lett.*, *36*, L07801, doi:10.1029/2008GL036797.
- 479 Huang, T. Y. W., and G. P. Brasseur (1993), Effect of long-term solar
480 variability in a two-dimensional interactive model of the middle atmo-
481 sphere, *J. Geophys. Res.*, *98*, 20,413–20,428.
- 482 Jones, H. P., T. L. Duvall, J. W. Harvey, C. T. Mahaffey, J. D. Schwitters,
483 and J. E. Simmons (1992), The NASA/NSO spectromagnetograph, *Sol.
484 Phys.*, *139*, 211–232.
- 485 Krivova, N. A., and S. K. Solanki (2005a), Reconstruction of solar UV
486 irradiance, *Adv. Space Res.*, *35*, 361–364.
- 487 Krivova, N. A., and S. K. Solanki (2005b), Modelling of irradiance variations
488 through atmosphere models, *Mem. Soc. Astron. Ital.*, *76*, 834–841.
- 489 Krivova, N. A., and S. K. Solanki (2008), Models of solar irradiance
490 variations: Current status, *J. Astrophys. Astron.*, *29*, 151–158.
- 491 Krivova, N. A., S. K. Solanki, M. Fligge, and Y. C. Unruh (2003), Reconstruc-
492 tion of solar total and spectral irradiance variations in cycle 23: Is solar
493 surface magnetism the cause?, *Astron. Astrophys.*, *399*, L1–L4.
- 494 Krivova, N. A., S. K. Solanki, and L. Floyd (2006), Reconstruction of solar
495 UV irradiance in cycle 23, *Astron. Astrophys.*, *452*, 631–639.
- 496 Langematz, U., J. L. Grenfell, K. Matthes, P. Mieth, M. Kunze, B. Steil, and
497 C. Brühl (2005a), Chemical effects in 11-year solar cycle simulations
498 with the Freie Universität Berlin Climate Middle Atmosphere Model with
online chemistry (FUB-CMAM-CHEM), *Geophys. Res. Lett.*, *32*, 499
L13803, doi:10.1029/2005GL022686.
- Langematz, U., K. Matthes, and J. L. Grenfell (2005b), Solar impact on
climate: Modeling the coupling between the middle and the lower atmo-
sphere, *Mem. Soc. Astron. Ital.*, *76*, 868–875.
- Lean, J. (2000), Evolution of the Sun's spectral irradiance since the Maunder
Minimum, *Geophys. Res. Lett.*, *27*, 2425–2428, doi:10.1029/
2000GL000043.
- Lean, J., G. Rottman, J. Harder, and G. Kopp (2005), SORCE contributions
to new understanding of global change and solar variability, *Sol. Phys.*,
230, 27–53, doi:10.1007/s11207-005-1527-2.
- Livingston, W. C., J. Harvey, C. Slaughter, and D. Trumbo (1976), Solar
magnetograph employing integrated diode arrays, *Appl. Opt.*, *15*, 40–52.
- Rottman, G. J., T. N. Woods, and T. P. Sparr (1993), Solar-stellar irradiance
comparison experiment: 1. Instrument design and operation, *J. Geophys.
Res.*, *98*, 10,667–10,677.
- Rožanov, E. V., M. E. Schlesinger, T. A. Egorova, B. Li, N. Andronova, and
V. A. Zubov (2004), Atmospheric response to the observed increase of
solar UV radiation from solar minimum to solar maximum simulated by
the University of Illinois at Urbana-Champaign climate-chemistry model,
J. Geophys. Res., *109*, D01110, doi:10.1029/2003JD003796.
- Rožanov, E., T. Egorova, W. Schmutz, and T. Peter (2006), Simulation of
the stratospheric ozone and temperature response to the solar irradiance
variability during Sun rotation cycle, *J. Atmos. Sol. Terr. Phys.*, *68*,
2203–2213.
- Scherrer, P. H., et al. (1995), The Solar Oscillations Investigation—Michelson
Doppler Imager, *Sol. Phys.*, *162*, 129–188.
- Solanki, S. K., N. A. Krivova, and T. Wenzler (2005), Irradiance models,
Adv. Space Res., *35*, 376–383.
- Tanaka, H., J. P. Castelli, A. E. Covington, A. Krüger, T. L. Landecker, and
A. Tlamicha (1973), Absolute calibration of solar radio flux density in the
microwave region, *Sol. Phys.*, *29*, 243–262.
- Unruh, Y. C., S. K. Solanki, and M. Fligge (1999), The spectral dependence
of facular contrast and solar irradiance variations, *Astron. Astrophys.*,
345, 635–642.
- Unruh, Y. C., N. A. Krivova, S. K. Solanki, J. W. Harder, and G. Kopp
(2008), Spectral irradiance variations: comparison between observations
and the SATIRE model on solar rotation time scales, *Astron. Astrophys.*,
486, 311–323.
- Viereck, R. A., L. E. Floyd, P. C. Crane, T. N. Woods, B. G. Knapp,
G. Rottman, M. Weber, L. C. Puga, and M. T. DeLand (2004), A
composite Mg II index spanning from 1978 to 2003, *Space Weather*,
2, S10005, doi:10.1029/2004SW000084.
- Wenzler, T., S. K. Solanki, N. A. Krivova, and D. M. Fluri (2004),
Comparison between KPVT/SPM and SoHO/MDI magnetograms with
an application to solar irradiance reconstructions, *Astron. Astrophys.*,
427, 1031–1043.
- Wenzler, T., S. K. Solanki, and N. A. Krivova (2005), Can surface magnetic
fields reproduce solar irradiance variations in cycles 22 and 23?, *Astron.
Astrophys.*, *432*, 1057–1061.
- Wenzler, T., S. K. Solanki, N. A. Krivova, and C. Fröhlich (2006), Reconstruc-
tion of solar irradiance variations in cycles 21–23 based on surface magnetic
fields, *Astron. Astrophys.*, *460*, 583–595.
- Wenzler, T., S. K. Solanki, and N. A. Krivova (2009), Reconstructed and
measured total solar irradiance: Is there a secular trend between 1978 and
2003?, *Geophys. Res. Lett.*, *36*, L11102, doi:10.1029/2009GL037519.
- Woods, T. N., et al. (1996), Validation of the UARS solar ultraviolet
irradiances: Comparison with the ATLAS 1 and 2 measurements, *J. Geo-
phys. Res.*, *101*, 9541–9570.
- Woods, T. N., W. K. Tobiska, G. J. Rottman, and J. R. Worden (2000),
Improved solar Lyman- α irradiance modeling from 1947 through 1999
based on UARS observations, *J. Geophys. Res.*, *105*, 27,195–27,215.
- N. A. Krivova, B. Podlipnik, and S. K. Solanki, Max-Planck-Institut für
Sonnensystemforschung, Max-Planck-Str. 2, D-37191 Katlenburg-Lindau,
Germany. (natalie@mpe.mpg.de)
- T. Wenzler, Hochschule für Technik Zürich, CH-8004 Zürich, Switzerland.